Multilayer White Organic Light-Emitting Diodes with Blue Fluorescent and Red Phosphorescent Materials

***Ji Hoon Seo*[1,2]**
[1]Dept. of Information Display, Hongik University, Seoul, Korea
[2]Center for Organic Materials and Information Devices,
Hongik University, Seoul, Korea

Jun Ho Kim*[2,3]*, Kum Hee Lee*[4]*, You-Hyun Kim*[5]*,
Woo Young Kim*[5]*, Seung Soo Yoon*[4]** and Young Kwan Kim*[1,2]**
[3]Dept. of Electronic Engineering, Hongik University, Seoul, Korea
[4]Dept. of Chemistry, Sungkyunkwan University, Suwon, Korea
[5]Dept. of Digital Display, Hoseo University, Asan, Korea

Phone: +82-2-320-1646, E-mail: kimyk@wow.hongik.ac.kr, ssyoon@skku.edu

Abstract

We have demonstrated highly efficient WOLED with two separated emissive layers using a blue fluorescent dye and a red phosphorescent dye. The maximum luminous efficiency of the device was 11.2 cd/A at 20 mA/cm^2 and CIE$_{x,y}$ coordinates varied from (x = 0.33, y = 0.37) at 6V to (x = 0.25, y = 0.33) at 14V.

1. Introduction

Organic light-emitting diodes (OLEDs) have drawn increasing attention in recent years.[1-2] Today, OLEDs are considered to be one of the flat-panel displays of the next generation due to low-voltage operation, wide-viewing angle, a high contrast and mechanical flexibility.[3] After Tang and VanSlyke firstly demonstrated new OLEDs with the structure of double layered organic materials between two electrodes, and numerous fluorescent materials, either material as host or dopant have been synthesized and developed.[4] It is hard to balance the holes and electrons in the emitting layer, because hole mobility is faster than electron mobility. Thus, multi-layered OLEDs (which consist of several layers such as HTL, ETL, EML, etc.) have been studied.[5]

White Organic light-emitting diodes (WOLEDs) have drawn increasing attention as a solid-state light source and backlights in liquid-crystal displays due to their light weight, low operating voltage and high contrast.[6-8] Thus the structures and materials for WOLEDs were extensively studied in many research groups.[9-12] One of the suggested WOLEDs consisted of one or two emissive layers with phosphorescent dyes.[13-14] But any blue phosphorescent material, in spite of their potential capacities, has not been considered yet as a proper candidate of WOLEDs due to their short lifetime and high energy gap causing difficulty in finding proper host materials. In this study, WOLEDs were fabricated with two emissive layers including a blue fluorescent dye and a red phosphorescent dye. The characteristics of WOLEDs depending on their thickness ratio of two emissive layers were investigated and the emission mechanism was also discussed.

2. Experiment

ITO coated glass was cleaned in an ultrasonic bath by regular sequence: in acetone, methanol, diluted water and isopropyl alcohol. Hereafter, pre-cleaned ITO was treated by O_2 plasma treatment whose condition were 2×10^{-2} Torr, 125 W and 2 min.[15] WOLEDs were fabricated using the high vacuum (5×10^{-7} Torr) thermal evaporation. As shown in Figure 1, the device structure was as follows: ITO / 4,4',4"-tris[2-naphthyl(phenyl)amino]triphenylamine (2-TNATA) as a hole injection layer / N,N′-bis-(1-naphyl)-N,N′-diphenyl-1,1′-biphenyl-4,4′-diamine (NPB) as a hole transport layer / blue dye doped in 2-methyl-9,10-di(2-naphthyl)anthracene (MADN) as a blue emissive layer / red dye doped in 4,4′-N,N′-dicarbazole-biphenyl (CBP) as a red emissive layer / 2,9-dimethy-4,7-

diphenyl-1,10-phenathorine (BCP) as an hole blocking layer / tris-(8-hydroxy-quinolinato) aluminum (Alq_3) as an electron transport layer / lithium quinolate (Liq) as an electron injection layer / aluminum (Al) as a cathode. Three kinds of the devices were fabricated and labeled as device 1, device 2 and device 3 which were contained by the different thick blue and red emissive layer as 25 nm and 5 nm, 27 nm and 3 nm and 28 nm and 2 nm, respectively. The UV/vis. and PL were measured with LS 50B. With the DC voltage bias, the optical and electrical properties of WOLEDs such as the current density, luminance, luminous efficiency and Commission Internationale de L'eclairage (CIE) coordinates characteristics were measured with keithley 236 and CHROMA METER CS-100A, respectively.

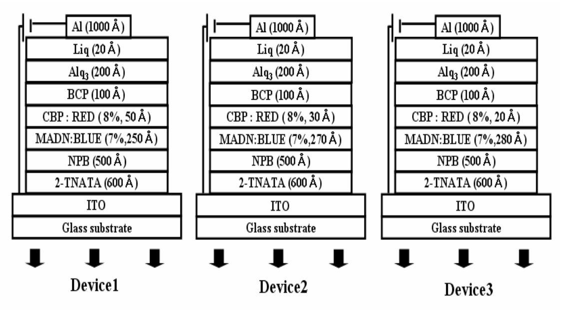

Fig. 1. The schemes of WOLEDs

3. Results and Discussion

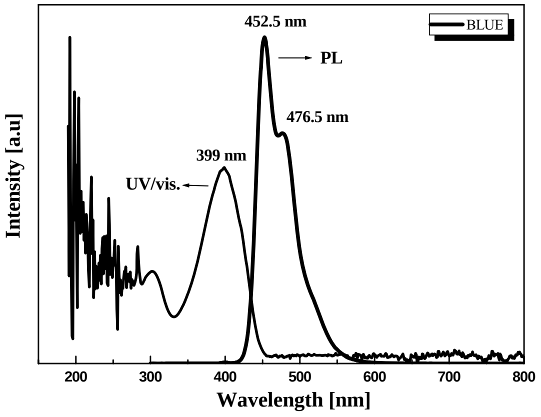

Fig. 2. UV/vis. absorption and PL spectrum of BLUE dopant used as blue emission

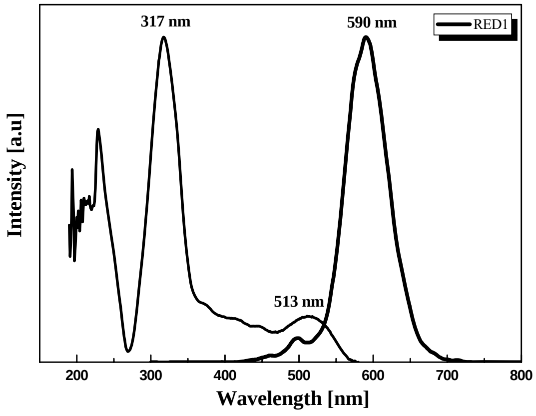

Fig. 3. UV/vis. absorption and PL spectrum of RED dopant used as red emission

Figure 2 and 3 show the UV/vis. absorption and PL spectra of BULE and RED dyes. The maximum UV/vis. absorption peaks of BLUE and RED dyes were 399 and 317 nm, respectively. As shown in Figure 3, the bands below 370 nm were assigned to the spin-allowed $^1\pi$- π^* transition of cyclometalated ligand, and the band around 430 nm can be assigned to spin-allowed metal-ligand charge transfer band (^{1}MLCT). Also, the band around 513 nm can be assigned to the spin-forbidden ^{3}MLCT band.

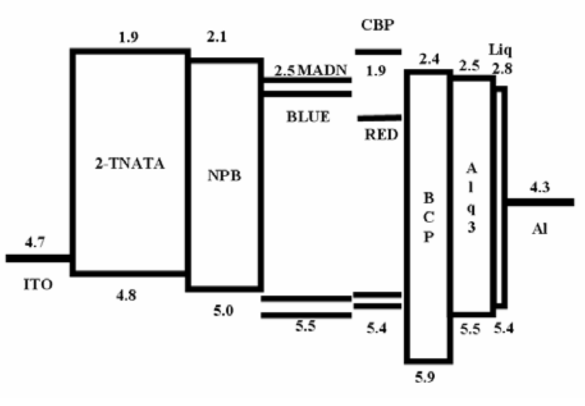

Fig. 4. The energy-level diagram of the WOLEDs in this works

Figure 4 shows the energy level diagram of the WOLEDs. The effectiveness of charge confinement relied on differences in the lowest unoccupied molecular orbital (LUMO) and the highest occupied molecular orbital (HOMO) levels between the EML and the adjacent layers. As shown in figure 4, the exciton was formed across the EML of MADN / EML of CBP interface and the 0.5 eV energy barrier between the HOMO of CBP at 5.4 eV and BCP at 5.9 eV act as an efficient barrier to hole transport across the EML/ETL interface.

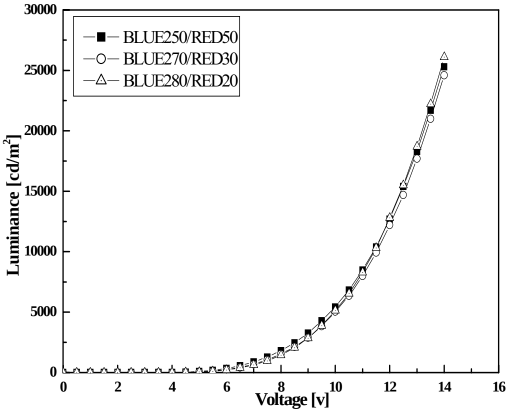

Fig. 5. The characteristics of luminance (L) versus voltage (V) in this works

Figure 5 shows the luminance versus the applied voltage with various thicknesses of emissive layers. Device 3 exhibited enhanced luminance characteristics at the high applied voltages, while device 1 showed better luminance at the low applied voltage region. The maximum luminance of device 3 was 26,100 cd/m^2 at 14 V.

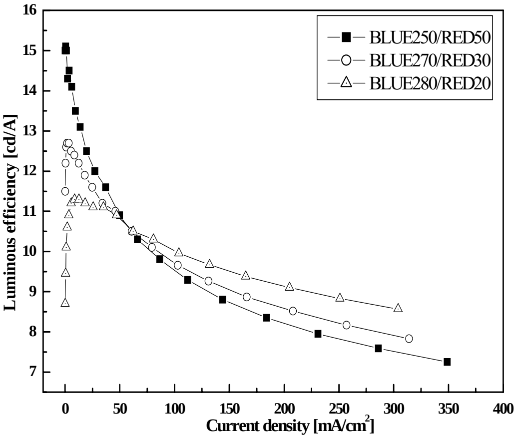

Fig. 6. The characteristics of luminous efficiency (LE) versus current density (J) in this works

Figure 6 shows the luminous efficiency versus current density on the devices. The luminous efficiency of device 1, 2 and 3 at the current density of 20 mA/cm^2 were 12.5, 11.9 and 11.2 cd/A, respectively. Device 1 and device 2 showed higher luminous efficiency than device 3 at the current density between 0 and 50 mA/cm^2, while the luminous efficiency of device 3 excelled those of the others above the current density of 50 mA/cm^2. Figure 7 shows CIE X and Y coordinates when the bias increased from 6 to 14 V. As shown in Figure 7, device 1 and 2 showed reddish white emission at the low voltage region, implying the strong red emission due to the improper thickness of the red emissive layer. As the thickness of the red emissive layer was decreased, the red emission intensity was also decreased causing the stable white color chromaticity.

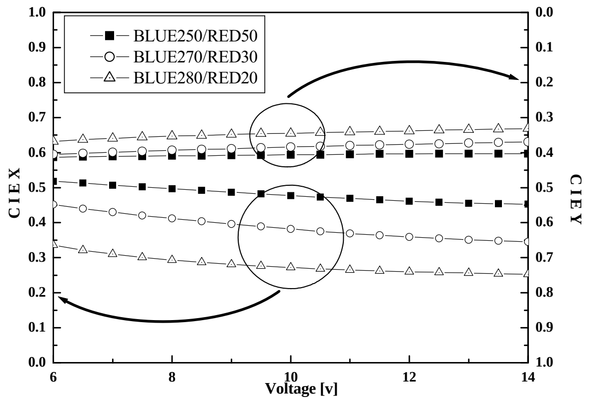

Fig. 7. The CIE$_{x,y}$ coordinates on the devices in this works

It was the reason why the device 3 exhibited the lower luminous efficiency than the others at the low current density as shown in Figure 6. Device 3 showed the color chromaticity close to the exact white emission (x = 0.33, y = 0.33) in CIE$_{x,y}$ coordinates as (x = 0.31, y = 0.36) at 7 V and exhibited the stable white emission from (x = 0.33, y = 0.37) to (x = 0.25, y = 0.33) at the operating voltages.

4. Conclusion

This work have demonstrated efficient WOLEDs with two separated emissive layers using a blue fluorescent dye and a red phosphorescent dye. The characteristics of the devices strictly depended on changing of the thickness of the blue and red emissive layers. Reducing the thickness of the red emissive layer caused the efficient and stable white emission at the high current densities. The device with the optimum structure showed the maximum luminance of 26,100 cd/m^2 at 14 V and the luminous efficiency of 11.2 cd/A at 20 mA/cm^2. Also it showed the stable white emission with CIE$_{x,y}$ coordinates from (0.33, 0.37) at 6V to (0.25, 0.33) at 14 V. We expect this result to solve a problem of making OLEDs backlight for thinner backlight unit.

5. Acknowledgements

This work was supported by a grant 10016748-2005-12 from Samsung Electronics.

References

[1] C.W. Tang, S.A. VanSlyke, Appl, Phys, Lett. **51**, 913 (1987)

[2] D.R. Baigen, N.C. Greenham, J. Gruener, R.N. Marks, R. H. Friend, S.C. Moratti, A.B. Holmes, Synth. Met. **67**, 3 (1994).

[3] R.F. Service, Science **273**, 878 (1996).

[4] C. W. Tang, S. A. VanSlyke and C. H. Chen, Appl. Phys. Lett. **65**, 913 (1989).

[5] C. Adachi, T.Tsutsui, and S. Saito, Appl. Phys. Lett. **57**, 531 (1987).

[6] Brian W. D'Andrade, Russell J. Holmes and Stephen R. Forrest, Adv. Mater. **16**, 624 (2004).

[7] Yao-Shan Wu, Shiao-Wen Hwang, Hsian-Hung Chen, Meng-Ting Lee, Wen-Jian Shen and chin H. Chen, Thin Solid Film, **488**, 165 (2005).

[8] Dashan Qin and Ye Tao, Appl. Phys. Lett. **86**, 113507 (2005).

[9] Brian W. D'Andrade and Stephen R. Forrest, Adv. Mater. **16**, 1585 (2004).

[10] M. A. Baldo, D. F. O'Brien, Y. You, A. Shoustikov, S. Sibley, M. E. Thompson and Stephen. R. Forrest, Nature (London), **395**, 151 (1998).

[11] Brian W. D'Andrade, Jason Brooks, Vadim Adamovich, Mark E. Thompson and Stephen R. Forrest, Adv. Mater. **14**, 1032 (2002).

[12] Jiu Yan Li, Di Liu, Chunwah Ma, Ondrej Lengyel, Chun-Sting Lee, Che-Ho Tung and Shuittong Lee, Adv. Mater. **16**, 1538 (2004).

[13] Gangtie Lei, Liduo Wang and Yong Qiu, Appl. Phys. Lett. **88**, 103508 (2006).

[14] B. W. D'Andrade, R. J. Holmes and S. R. Forrest, Adv. Mater. 16, 624 (2004).

[15] C. C. Wu, J. C. Sturm and A. Khan, Appl. Phys. Lett. **70**, 1348 (1997).